





Cite this: *RSC Adv.*, 2020, 10, 44712

# A pH-stable Ag(I) multifunctional luminescent sensor for the efficient detection of organic solvents, organochlorine pesticides and heavy metal ions†

Jianxin Ma, Yue Wang, Guocheng Liu,  Na Xu \* and Xiuli Wang \*

Developing novel luminescent materials for sensitive and rapid detection of heavy metal ions, organic solvents and organochlorine pesticides is vital for environmental monitoring. Herein, a new Ag(I) luminescent coordination polymer [Ag(3-dpyb)(H<sub>3</sub>odpa)]·H<sub>2</sub>O (LCP 1) (3-dpyb = *N,N'*-bis(3-pyridinecarboxamide)-1,4-butane, H<sub>4</sub>odpa = 4,4'-oxydiphthalic acid) was obtained by a hydrothermal reaction and characterized by single crystal, powder X-ray diffraction, infrared spectroscopy, thermogravimetric analysis and luminescence spectroscopy. LCP 1 is a three-dimensional (3D) supramolecular framework formed from 1D [Ag-3-dpyb-H<sub>3</sub>odpa]<sub>n</sub> chains and H-bond interactions. The luminescence sensing study of LCP 1 for recognizing organic solvents, organochlorine pesticides and heavy metal ions was performed, which demonstrated it to be a potential luminescent sensor for Hacac, NB, 2,6-DCN, Fe<sup>2+</sup>, Hg<sup>2+</sup>, and Fe<sup>3+</sup>. Fe<sup>2+</sup>, Hg<sup>2+</sup>, and Fe<sup>3+</sup> in river water were determined using LCP 1 with satisfying recovery.

Received 22nd October 2020  
Accepted 14th November 2020

DOI: 10.1039/d0ra08991e

rsc.li/rsc-advances

## Introduction

One of the serious problems troubling the scientific community today is the increasing pollution of our environment.<sup>1</sup> As documented in the literature, among the various pollutants, organic solvents, organochlorine pesticides, and heavy metal ions are seriously regarded as the main factors for environmental pollution. As one of the important chemical substances, small organic molecules play outstanding roles in human industrial production. However, chemicals such as acetylacetone (Hacac) and nitrobenzene (NB) are highly toxic and acutely carcinogenic, which can cause environmental pollution and threaten human health.<sup>2–5</sup> Therefore, rapid and selective detection of organic solvents is becoming urgent for environmental safety. In addition, the heavy demand for the production of cereals and vegetables leads to excessive use of organochlorine pesticides (OCPs) during planting. However, the high toxicity and slow degradation rate of OCPs have a negative impact on soil, water, and even human health even at very low concentrations.<sup>6,7</sup> Heavy metals are harmful to the health of virtually almost all living organisms.<sup>8</sup> In particular, heavy metal

ions, including Fe<sup>2+</sup>, Hg<sup>2+</sup>, and Fe<sup>3+</sup>, impose poisonous health effects attributed to oxidation substances formed in the body resulting in DNA damage and overall damage to the central nervous system.<sup>9,10</sup> Hence, it is of great significance to monitor the trace amount of these harmful pollutants to avoid the risk of pollution.

Currently, a variety of detection techniques have been reported, including liquid chromatography, gas chromatography, and electrochemical analysis.<sup>11–13</sup> However, these detection methods are expensive, complicated, and time-consuming. Thus, exploring and developing new detection technology to solve the above impediments are still a valuable academic issue of practical significance.<sup>14</sup> Recently, functional coordination polymers (CPs) have exhibited promising applications in many fields such as sensors, electronics, catalysis, and adsorption.<sup>15,16</sup> Especially, CPs have been considered as promising detection materials for trace contaminants due to their structural diversity.<sup>17</sup> Luminescent coordination polymers (LCPs) have attracted widespread attention because they can be employed as selective and sensitive probes for detecting pollutants. Regrettably, many LCPs can only aim to probe a single species, and it is very rare to detect multiple substances simultaneously with efficient performance.<sup>18</sup> Among various fluorescence sensors, LCPs containing Zn<sup>2+</sup>, Cd<sup>2+</sup> and Ag<sup>+</sup> have emerged as a novel type of fluorescent nanoprobe in chemical analysis. Especially, Ag(I) is an ideal luminescent material in the preparation of luminescent coordination polymers due to its strong coordination ability to nitrogen-donor atoms.<sup>19</sup> Many efforts to

College of Chemistry and Materials Engineering, Bohai University, Liaoning Professional Technology Innovation Center of Liaoning Province for Conversion Materials of Solar Cell, Jinzhou 121013, P. R. China. E-mail: xun872@bhu.edu.cn; wangxiuli@bhu.edu.cn

† Electronic supplementary information (ESI) available: Fig. S1–S16 and Tables S1–S11 (PDF). CCDC 2035795. For ESI and crystallographic data in CIF or other electronic format see DOI: 10.1039/d0ra08991e



develop luminescent chemosensors have been reported; however, only a few successful cases of silver(I) LCP are documented. Thus, it is still highly desirable to develop novel Ag fluorescent probes with improved stability and multifunctional detection ability.

Based on the above discussion, in this work, an Ag(I) coordination polymer (LCP **1**) was successfully synthesized by the hydrothermal reaction of *N,N'*-bis(3-pyridinecarboxamide)-1,4-butane (3-dpyb) and 4,4'-oxydipthalic acid ( $H_4odpa$ ) mixed ligands. LCP **1** is a 3D supramolecular framework constructed by 1D  $[Ag-3-dpyb-H_3odpa]_n$  chains and H-bond interactions. Notably, LCP **1** can be used as an optical sensor for the recognition of organic solvents, organochlorine pesticides and heavy metal ions.

## Experimental

### Materials and methods

The 3-dpyb ligand was prepared according to the literature method.<sup>20</sup> The reagents were commercially available and used directly without additional purification. The powder X-ray diffraction (PXRD) patterns were obtained at 40 kV, 40 mA with Cu K $\alpha$  ( $\lambda = 1.5406 \text{ \AA}$ ) radiation with a D/teX Ultra diffractometer and infrared spectra (IR) were acquired on a Varian 640 FTIR spectrometer with KBr discs. The thermogravimetric analysis (TGA) experiments were recorded on a Perkin-Elmer TGA analyzer. UV-vis absorption spectra were investigated through the Perkin Elmer Lambda 750. The fluorescence spectra were measured on a Hitachi F-4500 luminescence/phosphorescence spectrometer and the fluorescence lifetime curves were obtained on an FLS1000 Transient Steady-state Fluorescence Spectrometer.

### Synthesis of $[Ag(3-dpyb)(H_3odpa)] \cdot H_2O$ (**1**)

A mixture of  $AgNO_3$  (0.040 g, 0.2 mmol), 3-dpyb (0.030 g, 0.1 mmol),  $H_4odpa$  (0.035 g, 0.1 mmol),  $H_2O$  (9 mL) and 4 drops of  $HNO_3$  (1 M) were introduced into a Teflon-lined stainless-steel vessel (23 mL); the contents were allowed to react at  $120^\circ C$  for 4 days (Scheme S1<sup>†</sup>), after which it was cooled to room temperature. The colorless and transparent blocky crystals were collected by filtration, washed with  $H_2O$  and dried in air for 12 hours (yield of 69% based on Ag). Anal. calcd (%) for  $C_{32}H_{29}N_4AgO_{12}$ : C, 49.95; H, 3.79; N, 7.28. Found: C, 49.86; H, 3.72; N, 7.21. IR (KBr,  $cm^{-1}$ ): 3304 (s), 3072 (m), 2939 (m), 2871 (w), 2350 (w), 1662 (m), 1552 (s), 1482 (m), 1424 (w), 1370 (s), 1309 (m), 1265 (s), 1223 (s), 1135 (m), 1060 (w), 963 (s), 841 (m), 770 (s), 700 (s), 630 (m), 598 (m), 500 (w).

### Luminescence sensing study

The luminescence experiments of LCP **1** were proceeded *via* dispersing 2.5 mg solid samples in three types of analytical species to obtain suspensions by ultrasound; the fluorescence behavior of these suspensions were then observed by a luminescence spectrometer. For the first type of analytical species, LCP **1** was dispersed in the following different target organic solvents (3 mL): *N,N*-dimethylformamide (DMF), propyl alcohol (ProOH), *N,N*-dimethylacetamide (DMA), tetrahydrofuran

(THF), benzene (PhH), pyridine (Py), ethanol (EtOH), cyclohexane (CyH), methanol (MeOH), acetonitrile (ACN), iso-propyl alcohol (iso-ProOH), ethylene glycol (EG), dichloromethane (DCM), 1,4-diethylene dioxide (1,4-dioxane), dimethyl sulfoxide (DMSO), acetylacetone (Hacac) and nitrobenzene (NB). For the second type, different organochlorine pesticides were used as target analytes. Here, LCP **1** was added into  $10^{-3} \text{ mol L}^{-1}$  THF solutions with separately dissolved organochlorine pesticides, namely, carbaryl, atrazine, 1,2,4,5-tetrachlorobenzene (1,2,4,5-TetraCB), 2,6-dichloro-4-nitroaniline (2,6-DCN), 1,2,3-trichlorobenzene (1,2,3-TriCB), chlorobenzene (CB) and 1,3-dichlorobenzene (1,3-DCB), and then the mixtures were dispersed ultrasonically. LCP **1** was added to aqueous solutions containing different metal ions,  $M(NO_3)_x$  ( $M = Na^+, K^+, Mn^{2+}, Zn^{2+}, Cd^{2+}, Ba^{2+}, Mg^{2+}, Ca^{2+}, Fe^{2+}, Hg^{2+},$  and  $Fe^{3+}$ ) to obtain the third type of analytical species. The resulting concentration for the metal ions was  $10^{-3} \text{ mol L}^{-1}$  and then the mixtures containing LCP **1** and analytes were treated by ultrasonication for 1 h to form a stable suspension. Finally, the fluorescence behavior of the three types of suspensions were measured under an excitation of 345 nm for LCP **1**. The fluorescence intensity of the homogeneous suspension was frequently monitored.

## Results and discussion

### Crystal structure of LCP **1**

LCP **1** crystallizes in the triclinic system with  $P\bar{1}$  space group. The asymmetric unit of LCP **1** is constituted by one Ag(I) ion, one 3-dpyb ligand, and one incompletely deprotonated  $H_3odpa^-$  ligand (Fig. 1a). The central Ag(I) ion is three-coordinated by two N atoms from two 3-dpyb ligands and one carboxyl oxygen atom from one  $H_3odpa^-$  ligand. The length of the Ag–O bond is 2.721(7)  $\text{\AA}$ , which is similar to those previously reported.<sup>21</sup>

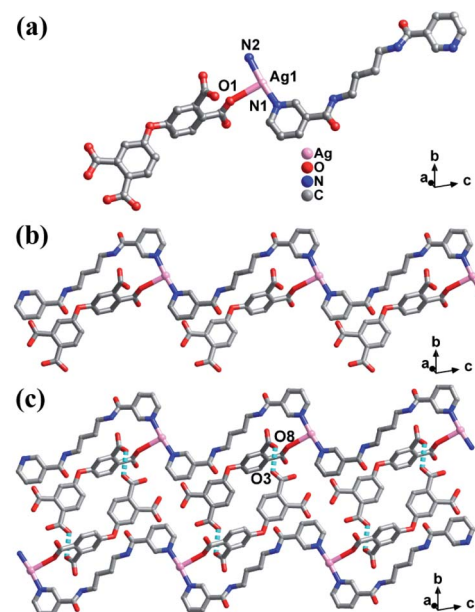


Fig. 1 (a) The coordination geometry of Ag atom in LCP **1**. (b) The 1D chain of LCP **1**. (c) The 2D supramolecular layered structure of LCP **1**.

In LCP **1**, the 3-dpyb ligands as linkers coordinated with Ag(I) ions to form a 1D [Ag-3-dpyb]<sub>n</sub> chain. Besides, incompletely deprotonated H<sub>3</sub>odpa<sup>−</sup> ligands hang on one side of the 1D [Ag-3-dpyb]<sub>n</sub> chains, which provide a prerequisite for three-dimensional (3D) supramolecular framework by H-bond interactions (Fig. 1b). Firstly, adjacent 1D chains were linked by H-bonding interactions [O(8)–H(8)···O(3)] with a length of 2.492 Å to form 2D supramolecular layers (Fig. 1c). The corresponding hydrogen-bonding parameters of LCP **1** are listed in Table S3.† Next, 2D layers were further connected through [O(5)–H(5)···O(2)] with a distance of 3.023 Å to form a 3D supramolecular structure (Fig. S1†).

### The thermogravimetric analyses (TGA), infrared spectroscopy (IR), and X-ray diffraction (PXRD) studies of LCP

The TGA curve of LCP **1** is elucidated in Fig. S2† under the N<sub>2</sub> atmosphere from 30 °C to 800 °C. LCP **1** showed a slow weight loss between 30 °C to 163 °C, followed by a weight loss of 2.33%, indicating the loss of one free H<sub>2</sub>O molecule (cal. 2.34%). From 193 °C to 325 °C, the rapid weight loss might be attributed to the decomposition of ligands. Then, with the increase of temperature, the framework collapsed and decomposed.

The IR spectra are displayed in Fig. S3,† which confirms the structural composition of LCP **1**. The peaks at 3304 cm<sup>−1</sup> are the stretching vibrations of O–H bonds in water.<sup>22</sup> The characteristic absorption peaks from 1680 to 1360 cm<sup>−1</sup> are attributed to the COO<sup>−</sup> group. The strong absorption peaks at 841 cm<sup>−1</sup>, 770 cm<sup>−1</sup>, and 700 cm<sup>−1</sup> are attributed to the ν(C–N) stretching vibrations of the N-heterocyclic rings.<sup>23</sup> The strong band at about 1662 cm<sup>−1</sup> was assigned to the ν(C=O) vibration of the amide groups.<sup>24</sup>

Since the stability of the fluorescent probe is critical in a sensing application, the PXRD patterns and the infrared spectrum of LCP **1** were obtained under different conditions. The PXRD patterns of the synthesized samples are exhibited in Fig. S5,† which indicated that the crystallinity and phase purity of LCP **1** were good in different conditions. The samples of LCP **1** were particularly placed in air for about 6 months to determine if the samples were stable. The results showed that the PXRD peak of LCP **1** was consistent with that of the fresh one, indicating the excellent stability of LCP **1**. Moreover, the infrared spectra of LCP **1** under various conditions were further investigated. It can be seen from Fig. S4† that the absorption peaks of the samples were almost unchanged. These results collectively demonstrated that LCP **1** has great stability, which gave us reason to further conduct luminescence experiments.

### Solid fluorescence spectra of LCP **1**

To investigate the luminescence properties of LCP **1**, the excitation and emission spectra in the solid state were measured in open-air conditions. As shown in Fig. S6,† the emission spectrum shows a peak at 405 nm under an excitation of 345 nm, which may be due to ligand-to-metal charge transfer (LMCT).<sup>25</sup>

### Sensing of organic solvents

Considering the high stability and obvious fluorescence properties of LCP **1** in water, we firstly explored their potential ability to sense organic solvents at room temperature and pressure.

LCP **1** (2.5 mg) was dispersed in 4 mL solvents, and the suspensions were formed by ultrasonication. Herein, seventeen common organic solvents, namely, DMF, ProOH, DMA, PhH, THF, Py, EtOH, CyH, MeOH, ACN, iso-ProOH, EG, DCM, 1,4-dioxane, DMSO, Hacac and NB were selected as representatives to investigate their influence on the luminescence properties of LCP **1**. Interestingly, the addition of different organic solvents induced diverse changes in the fluorescence intensity compared with the blank experiment. As shown in Fig. 2a and Fig. S11,† the luminescence intensity of LCP **1** showed a dramatic quenching effect by the addition of Hacac and NB within 15 seconds.

To further explore the sensing sensitivity of LCP **1** to Hacac and NB, the concentration gradient experiment was carried out with Hacac and NB. The concentrations were adjusted by EtOH ranging from 0 to 3.0 mM for Hacac and 0 to 2.6 mM for NB. As displayed in Fig. 3a and b, the luminescence intensities gradually decreased with an increase in Hacac and NB concentration. The luminescence-quenching efficiency was described by the Stern–Volmer (S–V) equation,<sup>26</sup>  $I_0/I = 1 + K_{sv} \times [C]$ , where  $I_0$  and  $I$  refer to the luminescence intensities of LCP **1** before and after sensing Hacac or NB,  $K_{sv}$  is the constant and  $[C]$  represents the concentrations of Hacac or NB (Fig. 3c and d). The correlation coefficients ( $R^2$ ) are 0.9965 for Hacac and 0.9993 for NB.  $K_{sv}$  of LCP **1** are  $1.542 \times 10^4 \text{ M}^{-1}$  and  $1.683 \times 10^4 \text{ M}^{-1}$  for Hacac

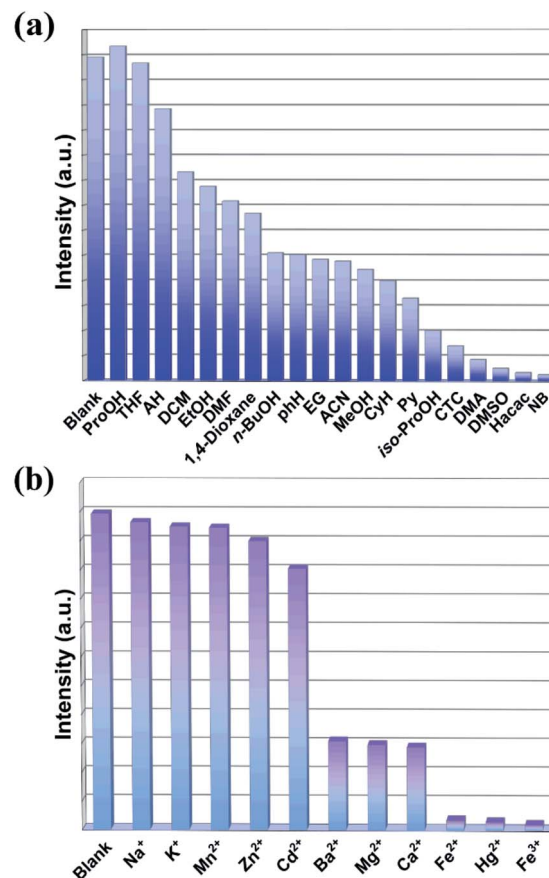


Fig. 2 Fluorescence emission intensities of LCP **1** dispersed in different organic solvents (a), and in the presence of different metal ions (b).





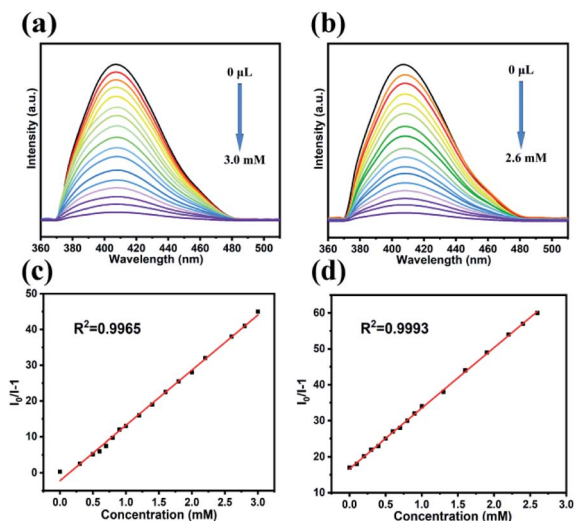


Fig. 3 Luminescence titration of LCP 1 at different concentrations of Hacac (a) and NB (b). The S–V plot of LCP 1 at different concentrations of Hacac (c) and NB (d) in EtOH.

and NB, respectively, according to the corresponding S–V plots. The detection limit is calculated with  $3\delta/K_{SV}$ ;  $\delta$  represents the blank standard deviation for ten times, as illustrated in Fig. S7.† So the detection limit for Hacac and NB are  $1.517 \times 10^{-5}$  M and  $1.391 \times 10^{-5}$  M, respectively, indicating that LCP 1 can efficiently detect Hacac and NB. The  $K_{SV}$  and detection limit values for LCP 1 are comparable to those of the CPs reported in the literature (Tables S4 and S5†).<sup>10,27–32</sup>

The sensing selectivity of LCP 1 for Hacac or NB in the presence of other interferential analytes (including DMF, ProOH, DMA, PhH, THF, Py, EtOH, CyH, MeOH, ACN, iso-ProOH, EG, DCM, 1,4-dioxane, and DMSO) were evaluated. First, equal amount of interferents were mixed to form a mixture. Then, LCP 1 (2.5 mg) was dispersed in 4 mL H<sub>2</sub>O to form a suspension solution; the above interferent mixture was first added followed by Hacac or NB solution. Finally, the corresponding emissions were monitored. As shown in Fig. S8,† the emission intensity of LCP 1 was quenched by 35% or 28% in the presence of the interferent mixture. Upon introducing the mixture of Hacac or NB and the interferents, the fluorescence of the system was quenched strongly. This suggests the high selectivity of LCP 1 towards Hacac and NB despite the existence of interferents.

The recycling performance is vital for a good sensor. To further illustrate the cyclic detection performances of LCP 1 on Hacac and NB, the recycling performance were carried out. After quenching–recovery cycles, the luminescence intensity was well retained. The experimental results indicated that LCP 1 basically remained unchanged for at least five runs (Fig. S13a and b†). Besides, the PXRD pattern of the samples after five detections could still match well to that of the as-synthesized samples, showing that LCP 1 has excellent stability (Fig. S13d and e†).

### Sensing of organochlorine pesticides (OCPs)

OCPs are widely used in agriculture. Although the growth of plants requires the use of pesticides, excessive use has caused

an enormous detrimental effect on water and even human health. Therefore, the selective sensing of OCPs in solution at room temperature and pressure was studied in this work. Seven pesticides were selected, namely, carbaryl, atrazine, 1,2,4,5-TetraCB, 2,6-DCN, 1,2,3-TriCB, CB and 1,3-DCB. Besides, the fluorescence emission spectra of fluorophores are frequently found to be sensitive to the polarity of the solvent environment. Therefore, the impact on the emission of LCP 1 was first analyzed; an optimal solvent was identified for OCP detection after soaking LCP 1 in diverse organic solvents for 24 h. Fortunately, when dispersed in THF, the emission spectrum was basically the same as that of LCP 1 in water (Fig. S11†). The subsequent experimental methods were the same as that used for sensing the organic solvents apart from changing the solvent to THF. The resulting concentration for the OCPs was  $10^{-3}$  mol L<sup>−1</sup>. Fig. 4a shows the changes in the fluorescence intensity after adding LCP 1 to the THF solvent containing seven different types of OCPs. The results showed that 2,6-DCN had a significant fluorescence quenching effect on LCP 1.

The fluorescence intensities of LCP 1 for different pesticides were recorded, and is shown in Fig. 4b. After adding 2,6-DCN, the luminescence intensity was quenched in a short time (15 s) and the quenching efficiency reached 92%. However, the fluorescence intensity had little change after the addition of all OCPs except for 2,6-DCN. In order to understand the constant values, fluorimetric titrations were performed with 2,6-DCN, where the relationship between the  $I_0/I$  and concentration was studied (Fig. 4c). The  $K_{SV}$  value is  $2.028 \times 10^5$  M<sup>−1</sup> for 2,6-DCN. The detection limit calculated by  $3\delta/K_{SV}$  is  $1.154 \times 10^{-6}$  M (Fig. S12†). The  $K_{SV}$  and detection limit values for LCP 1 are similar to those of the CPs reported in the literature (Table S6†).<sup>33–36</sup>

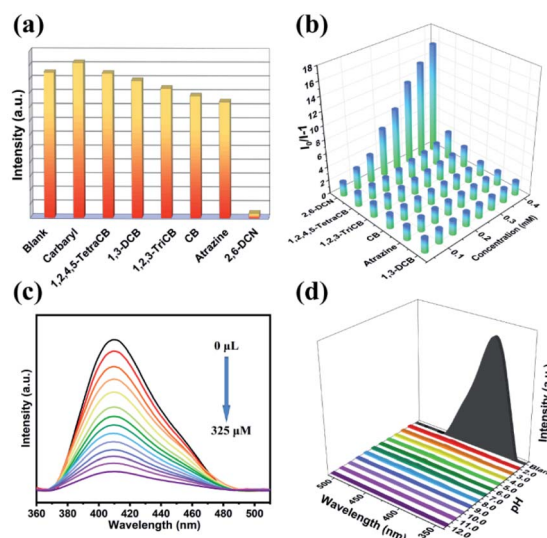


Fig. 4 (a) Fluorescence intensity of LCP 1 dispersed in OCPs. (b) The fluorescence intensity of  $I_0/I$  of LCP 1 vs. the concentration of various pesticides. (c) Luminescence titration of LCP 1 at different concentrations of 2,6-DCN in THF solution. (d) The luminescence intensity in the pH range of 2.0–12.0 of 2,6-DCN.

Besides, agricultural pollutants are quite complicated; there are many forms of contaminants that coexist in different pH solutions, and hence a 2,6-DCN luminescence sensor with high stability is urgently required. Bearing in mind the above considerations, we conducted the luminescence-quenching stability test of 2,6-DCN within the pH range of 2.0–12.0 (adjust the pH by dropping 0.1 M HNO<sub>3</sub> or 0.1 M NaOH in 10<sup>−3</sup> mol L<sup>−1</sup> THF solution of 2,6-DCN and then add 2.5 mg of LCP 1). From Fig. 4d, it can be seen that with the change in pH values, the quenching intensity of 2,6-DCN remains good. Thus, LCP 1 can be used as a highly selective sensor for detecting 2,6-DCN in THF solutions. More importantly, the fluorescence quenching mechanism of 2,6-DCN was inactive on other pesticides present in the solution, as demonstrated by competitive experiments (Fig. S9†). Simultaneously, the recyclability study of LCP 1 on 2,6-DCN has been carried out. After five cycles, the luminescence intensity only decreased slightly compared with the original one. The PXRD patterns further proved that the initial framework was not destroyed, reflecting the good regeneration ability of LCP 1 (Fig. S13c and f†).

### Sensing of metal ions

The strong emission and good water stability of LCP 1 prompted us to study its luminescence sensing characteristics. To verify the potential of LCP 1 for sensing metal ions, 2.5 mg samples of LCP 1 were firstly dispersed into 3 mL solution (1 × 10<sup>−3</sup> M) containing Na<sup>+</sup>, K<sup>+</sup>, Mn<sup>2+</sup>, Zn<sup>2+</sup>, Cd<sup>2+</sup>, Ba<sup>2+</sup>, Mg<sup>2+</sup>, Ca<sup>2+</sup>, Fe<sup>2+</sup>, Hg<sup>2+</sup>, or Fe<sup>3+</sup>; all relevant experiments were tested at room temperature and pressure.

Then, the mixed solutions were subjected to ultrasonic vibration for half an hour to form a series of suspensions; finally, the detection studies were executed.

As shown in Fig. 2b, Na<sup>+</sup>, K<sup>+</sup>, Mn<sup>2+</sup>, Zn<sup>2+</sup> and Cd<sup>2+</sup> had a minor effect on the luminescence intensity. Ba<sup>2+</sup>, Mg<sup>2+</sup>, and Ca<sup>2+</sup> had a slight inhibition on the luminescence of LCP 1. Obviously, LCP 1 undergoes more intense fluorescence quenching with Fe<sup>2+</sup>, Hg<sup>2+</sup>, and Fe<sup>3+</sup>. It implies that LCP 1 can be counted as a potential candidate for probing Fe<sup>2+</sup>, Hg<sup>2+</sup>, and Fe<sup>3+</sup>. Moreover, fluorimetric titrations were performed to explore the interaction constant values. As the concentration of metal ions increases, the fluorescence intensity decreases regularly (Fig. 5). LCP 1 showed a fast quenching within 15 s towards Fe<sup>2+</sup>, Hg<sup>2+</sup> and Fe<sup>3+</sup> ions in the aqueous solution, and the quenching efficiency remained unchanged for 5 minutes. The quenching of the fluorescence intensity of LCP 1 was further analyzed with the help of the Stern–Volmer equation. The *K*<sub>sv</sub> value for Fe<sup>2+</sup>, Hg<sup>2+</sup>, and Fe<sup>3+</sup> were found to be 6.107 × 10<sup>4</sup> M<sup>−1</sup>, 1.005 × 10<sup>5</sup> M<sup>−1</sup>, and 1.186 × 10<sup>5</sup> M<sup>−1</sup>, respectively. The limit of detection for Fe<sup>2+</sup>, Hg<sup>2+</sup>, and Fe<sup>3+</sup> were 3.831 × 10<sup>−6</sup> M, 2.328 × 10<sup>−6</sup> M, and 1.973 × 10<sup>−6</sup> M, respectively, in water. There are reports in the literature where the detection of Fe<sup>2+</sup>, Hg<sup>2+</sup>, and Fe<sup>3+</sup> has been recorded in both organic and water media (Tables S7–S9†).<sup>10,30,37–49</sup> Compared with these examples reported, LCP 1 demonstrated impressive results.

Furthermore, five cycles of the Fe<sup>2+</sup>, Hg<sup>2+</sup>, and Fe<sup>3+</sup> sensing experiments were performed. The collected results showed that

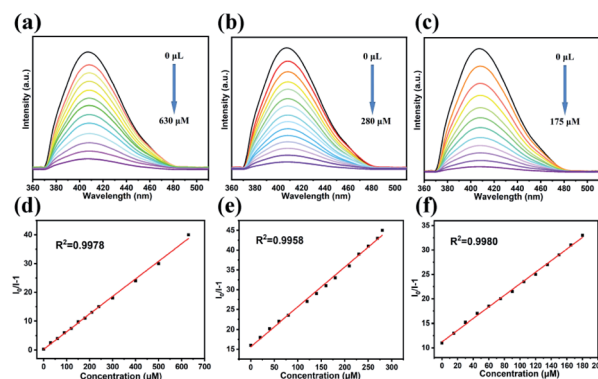


Fig. 5 Fluorescence spectra of LCP 1 dispersed in different concentrations of Fe<sup>2+</sup> (a), Hg<sup>2+</sup> (b) and Fe<sup>3+</sup> (c). The S–V plot of LCP 1 at different concentrations of Fe<sup>2+</sup> (d), Hg<sup>2+</sup> (e) and Fe<sup>3+</sup> (f).

LCP 1 could recover its luminescence intensity after washing several times (Fig. S14†). The competition experiments showed that the presence of other metal ions did not interfere with the fluorescence responses of Fe<sup>2+</sup>, Hg<sup>2+</sup>, and Fe<sup>3+</sup>. The results revealed that LCP 1 can detect Fe<sup>2+</sup>, Hg<sup>2+</sup>, and Fe<sup>3+</sup> with remarkable selectivity (Fig. S10†). Thus, it can be presumed that LCP 1 can be used as a potentially stable and highly selective probe for the detection of Fe<sup>2+</sup>, Hg<sup>2+</sup>, and Fe<sup>3+</sup> in water. To verify the practicality of LCP 1, fluorescence detection experiments on river water samples containing Fe<sup>2+</sup>, Hg<sup>2+</sup>, and Fe<sup>3+</sup> were performed. The water samples were obtained from a local river (Table S10†). After simple filtration and separation, Fe<sup>2+</sup>, Hg<sup>2+</sup>, or Fe<sup>3+</sup> were not detected in the river water samples. To confirm the validity of the present work, three different concentrations (5, 10 and 15 μM) of Fe<sup>2+</sup>, Hg<sup>2+</sup>, or Fe<sup>3+</sup> ions were added to LCP 1 at three different concentrations (5, 10 and 15 μM) to the river water samples for performing the standard addition recovery experiments. The recovery values of water samples were 96.2–100.20%, 99.73–102.20%, and 100.06–104.33%, respectively. The results suggested that LCP 1 had great practicability for the determination of metal ions in the environment.

### The time-dependent tests on fluorescence emission response

Time-dependent fluorescence emission response experiments were conducted by adding 50 μL of analytes (Hacac, NB, 2,6-DCN, Fe<sup>2+</sup>, Hg<sup>2+</sup>, and Fe<sup>3+</sup>) to a 3 mL dispersion of LCP 1. As shown in Fig. S16,† the intensity evidently decreased in a short time (15 s), leading to a significant increase in the quenching efficiency, which reveals that LCP 1 is sensitive and is a rapid sensor towards Hacac, NB, 2,6-DCN, Fe<sup>2+</sup>, Hg<sup>2+</sup>, and Fe<sup>3+</sup>.

### Sensing mechanism

The possible quenching mechanism in CPs generally includes the following points: (i) structural collapse of the CP framework, (ii) a weak coordinating interaction of analytes with the framework, and (iii) competitive adsorption between the framework and the analytes.<sup>50–52</sup> In order to determine the possible quenching mechanism in this work, initially, we examined the coherence of the PXRD patterns between LCP 1



after luminescence research and the simulated one. The results demonstrated that the framework remained stable; so the luminescence quenching is not due to the collapse of the framework (Fig. S4†). The second possibility was also ruled out because comparing the IR spectra (Fig. S3†) before and after the sensing process, it was found that there was no obvious peak position or intensity change, that is to say, no new interactions were generated. Therefore, Forster resonance energy transfer (FRET) might play an important role in the detection of these analytes. We studied the overlap between the absorption and emission spectra for each analyte and the sensing species. The UV-vis absorption spectra of twelve analytes and the emission spectrum of LCP 1 were investigated (Fig. 6). The strong absorption bands from the UV-visible absorption spectra of 2,6-DCN,  $\text{Fe}^{2+}$ ,  $\text{Hg}^{2+}$ , and  $\text{Fe}^{3+}$  show a great overlap with the emission spectrum of LCP 1; however, there is almost no obvious overlap between the emission spectrum of LCP 1 and the absorption spectra of Hacac and NB, demonstrating that these analytes are not completely gratified with the energy competition absorption. So, energy transfer may not be the only mechanism.

In order to further confirm the fluorescence mechanism, the fluorescence average lifetime measurements based on the suspension solution of LCP 1 were carried out before and after the addition of analytes. Notably, the lifetime decay curves of LCP 1 before and after exposure to analytes showed only an inappreciable variation, which indicated that the quenching mechanism was more inclined to static quenching (Fig. S15†). Conversely, compared with the original curve, the fluorescence lifetime had an obvious change, which belonged to a dynamic annihilation process. For LCP 1, the lifetime value was 7.948 ns. After adding analytes, the average lifetime values were 7.959 ns (adding Hacac) and 7.963 ns (adding NB). The changes in the average lifetime value indicated that static quenching was the primary pathway in the fluorescence quenching process of the organic solvents.

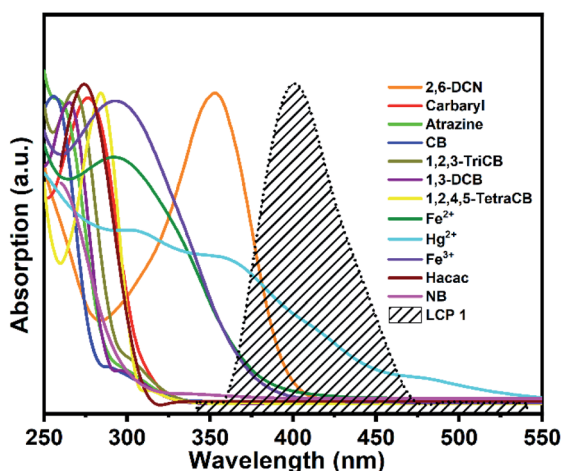


Fig. 6 UV-vis optical absorption spectra of analytes along with the emission spectrum of LCP 1 (dotted black line).

## Conclusions

In conclusion, a novel luminescent 3D Ag(I) supramolecular framework was successfully constructed from a tetradentate carboxylate ligand ( $\text{H}_4\text{odpa}$ ) and flexible bis(pyridyl)bis(amide) (3-dpyb) under hydrothermal conditions. This stable framework exhibits prominent fluorescence sensing properties for the selective detection of Hacac, NB, 2,6-DCN,  $\text{Fe}^{2+}$ ,  $\text{Hg}^{2+}$ , and  $\text{Fe}^{3+}$  with the advantages of low detection limit. Moreover, LCP 1 also exhibited good reproducibility and long-term stability. In the pH range of 2.0–12.0, LCP 1 could still maintain excellent sensing effect on 2,6-DCN. Thus, LCP 1 was used as a sensor for detecting  $\text{Fe}^{2+}$ ,  $\text{Hg}^{2+}$ , and  $\text{Fe}^{3+}$  in river water with satisfactory recovery. Furthermore, the reason for the fluorescence quenching of LCP 1 on 2,6-DCN,  $\text{Fe}^{2+}$ ,  $\text{Hg}^{2+}$ , and  $\text{Fe}^{3+}$  was related to the FRET mechanism, while Hacac and NB leading to the fluorescence quenching of LCP 1 was ascribed to static quenching. Therefore, LCP 1 can be considered as an eminently potential competitive and reliable candidate for the detection of organic solvents, organochlorine pesticides and heavy metal ions.

## Conflicts of interest

There are no conflicts to declare.

## Acknowledgements

The acknowledgements come at the end of an article after the conclusions and before the notes and references. This work was financially supported by the National Natural Science Foundation of China (No. 21971024, 21671025) and Liao Ning Revitalization Talents Program (XLYC1902011).

## References

- 1 K. Remoundou and P. Koundouri, *Int. J. Environ. Res. Public Health*, 2009, **6**, 2160–2178.
- 2 X. M. Kang, X. Y. Fan, P. Y. Hao, W. M. Wang and B. Zhao, *Inorg. Chem. Front.*, 2019, **6**, 271–277.
- 3 D. Yang, L. Lu, S. Feng and M. Zhu, *Dalton Trans.*, 2020, **49**, 7514–7524.
- 4 J. Q. Liu, Z. D. Luo, Y. Pan, A. Kumar Singh, M. Trivedi and A. Kumar, *Coord. Chem. Rev.*, 2020, **406**, 213145.
- 5 L. Esrafil, F. D. Firuzabadi, A. Morsali and M. L. Hu, *J. Hazard. Mater.*, 2021, **403**, 123696.
- 6 G. Chakraborty, P. Das and S. K. Mandal, *ACS Appl. Mater. Interfaces*, 2018, **10**, 42406–42416.
- 7 C. L. Tao, B. Chen, X. G. Liu, L. J. Zhou, X. L. Zhu, J. Cao, Z. G. Gu, Z. Zhao, L. Shen and B. Z. Tang, *Chem. Commun.*, 2017, **53**, 9975–9978.
- 8 J. Cepeda and A. R. Diéguez, *CrystEngComm*, 2016, **18**, 8556–8573.
- 9 G. C. Liu, Y. Li, J. Chi, N. Xu, X. L. Wang, H. Y. Lin and Y. Q. Chen, *Dyes Pigm.*, 2020, 174.
- 10 J. X. Ma, N. Xu, Y. Liu, Y. Wang, H. Li, G. C. Liu, X. L. Wang and J. R. Li, *Inorg. Chem.*, 2020, **59**, 15495–15503.

- 11 C. Miao, *Inorg. Chem. Commun.*, 2019, **105**, 86–92.
- 12 B. Wang, X. L. Lv, D. Feng, L. H. Xie, J. Zhang, M. Li, Y. Xie, J. R. Li and H. C. Zhou, *J. Am. Chem. Soc.*, 2016, **138**, 6204–6216.
- 13 K. Ren, S. H. Wu, X. F. Guo and H. Wang, *Inorg. Chem.*, 2019, **58**, 4223–4229.
- 14 Y. Wang, S. H. Xing, F. Y. Bai, Y. H. Xing and L. X. Sun, *Inorg. Chem.*, 2018, **57**, 12850–12859.
- 15 A. J. Liu, F. Xu, S. D. Han, J. Pan and G. M. Wang, *Cryst. Growth Des.*, 2020, **20**, 7350–7355.
- 16 M. Cao, R. Pang, Q. Y. Wang, Z. Han, Z. Y. Wang, X. Y. Dong, S. F. Li, S. Q. Zang and T. C. W. Mak, *J. Am. Chem. Soc.*, 2019, **141**, 14505–14509.
- 17 K. C. Stylianou, R. Heck, S. Y. Chong, J. Bacsá, J. T. A. Jones, Y. Z. Khimiyak, D. Bradshaw and M. J. Rosseinsky, *J. Am. Chem. Soc.*, 2010, **132**, 4119–4130.
- 18 C. X. Yang, H. B. Ren and X. P. Yan, *Anal. Chem.*, 2013, **85**, 7441–7446.
- 19 J. Z. Huo, X. M. Su, X. X. Wu, Y. Y. Liu and B. Ding, *CrystEngComm*, 2016, **18**, 6640–6652.
- 20 Y. F. Hsu, C. H. Lin, J. D. Chen and J. C. Wang, *Cryst. Growth Des.*, 2008, **8**, 1094–1096.
- 21 L. Brammer, M. D. Burgard, M. D. Eddleston, C. S. Rodger, N. P. Rath and H. Adams, *CrystEngComm*, 2002, **4**, 239–248.
- 22 X. L. Wang, B. Mu, H. Y. Lin and G. C. Liu, *J. Organomet. Chem.*, 2011, **696**, 2313–2321.
- 23 B. Dolenský, R. Konvalinka, M. Jakubek and V. Král, *J. Mol. Struct.*, 2013, **1035**, 124–128.
- 24 L. Yang, F. Wang, D. Y. Auphedeous and C. Feng, *Nanoscale*, 2019, **11**, 14210–14215.
- 25 X. L. Wang, Y. Xiong, X. T. Sha, G. C. Liu and H. Y. Lin, *Cryst. Growth Des.*, 2017, **17**, 483–496.
- 26 J. Keizer, *J. Am. Chem. Soc.*, 1983, **105**, 1494–1498.
- 27 Q. Q. Xiao, G. Y. Dong and Y. H. Li, *Inorg. Chem.*, 2019, **58**, 15696–15699.
- 28 X. M. Kang, X. Y. Fan and P. Y. Hao, *Inorg. Chem. Front.*, 2019, **6**, 271–277.
- 29 S. L. Yao, S. J. Liu, X. M. Tian, T. F. Zheng, C. Cao, C. Y. Niu, Y. Q. Chen and H. R. Wen, *Inorg. Chem.*, 2019, **58**, 3578–3581.
- 30 B. L. Martinez, A. D. Shrode, R. J. Staples and R. L. LaDuca, *Polyhedron*, 2018, **151**, 369–380.
- 31 X. Wang, Y. Han and X. X. Han, *New J. Chem.*, 2018, **42**, 19844–19852.
- 32 X. D. Duan, F. Y. Ge and H. G. Zheng, *Inorg. Chem. Commun.*, 2019, **107**, 107479.
- 33 G. C. Liu, S. W. Han, Y. Gao, N. Xu, X. L. Wang and B. K. Chen, *CrystEngComm*, 2020, **22**, 7952–7961.
- 34 D. D. Feng, Y. D. Zhao, X. Q. Wang, D. D. Fang, J. Tang, L. M. Fan and J. Yang, *Dalton Trans.*, 2019, **48**, 10892–10900.
- 35 N. Xu, Q. H. Zhang, B. S. Hou, Q. Cheng and G. A. Zhang, *Inorg. Chem.*, 2018, **57**, 13330–13340.
- 36 H. He, S. H. Chen, D. Y. Zhang, R. Hao, C. Zhang, E. C. Yang and X. J. Zhao, *Dalton Trans.*, 2017, **46**, 13502–13509.
- 37 C. F. Wan, Y. J. Chang, C. Y. Chien, Y. W. Sie, C. H. Hu and A. T. Wu, *J. Lumin.*, 2016, **178**, 115–120.
- 38 N. Lashgari, A. Badiei and G. Mohammadi Ziarani, *J. Fluoresc.*, 2016, **26**, 1885–1894.
- 39 S. Çetindere, S. O. Tümay, *et al.*, *J. Fluoresc.*, 2016, **26**, 1173–1181.
- 40 S. Pandey, A. Azam, S. Pandey and H. M. Chawla, *Org. Biomol. Chem.*, 2009, **7**, 269–279.
- 41 S. A. A. Razavi, M. Y. Masoomi and A. Morsali, *Inorg. Chem.*, 2017, **56**, 9646–9652.
- 42 M. G. Choi, Y. H. Kim, J. E. Namgoong and S. K. Chang, *Chem. Commun.*, 2009, **24**, 3560–3562.
- 43 K. Xu, Y. Li, Y. Si, Y. He, J. Ma, J. He, H. Hou and K. A. Li, *J. Lumin.*, 2018, **204**, 182–188.
- 44 R. M. Tivier, I. Leray, B. Lebeau and B. Valeurab, *J. Mater. Chem.*, 2005, **15**, 2965–2973.
- 45 Z. Zhan, X. Liang, X. Zhang, Y. Jia and M. Hu, *Dalton Trans.*, 2019, **48**, 1786–1794.
- 46 X. Y. Guo, Z. P. Dong, F. Zhao, Z. L. Liu and Y. Q. Wang, *New J. Chem.*, 2019, **43**, 2353–2361.
- 47 Y. Li, Z. Chang, F. Huang, P. Wu, H. Chu and J. Wang, *Dalton Trans.*, 2018, **47**, 9267–9273.
- 48 M. Zheng, H. Tan, Z. Xie, L. Zhang, X. Jing and Z. Sun, *ACS Appl. Mater. Interfaces*, 2013, **5**, 1078–1083.
- 49 B. Wang, Q. Yang, C. Guo, Y. Sun, L. H. Xie and J. R. Li, *ACS Appl. Mater. Interfaces*, 2017, **9**, 10286–10295.
- 50 Y. K. Fan, W. Y. Zhang, S. S. Zhang, Y. T. Yan, K. Zhong, Y. Zhang, G. P. Yang and Y. Y. Wang, *J. Solid State Chem.*, 2019, **269**, 386–395.
- 51 Y. T. Yan, W. Y. Zhang, F. Zhang, F. Cao, R. F. Yang, Y. Y. Wang and L. Hou, *Dalton Trans.*, 2018, **47**, 1682–1692.
- 52 S. Y. Zhu and B. Yan, *Dalton Trans.*, 2018, **47**, 11586–11592.

